PCCP

Accepted Manuscript

ROYAL SOCIETY OF CHEMISTRY

www.rsc.org/pccp

Phys. Chem. Chem. Phys.

Cite this: DOI: 10.1039/c0xx00000x

www.rsc.org/xxxxxx

View Article Online
DOI: 10.1039/C5CP00696A

ARTICLE TYPE

Bent-core liquid crystalline cyanostilbenes: fluorescence switching and thermochromism

Marta Martínez-Abadía,[a] Shinto Varghese,[b,c] Begoña Milián-Medina,[b,d] Johannes Gierschner,[b] Raquel Giménez,[a] M. Blanca Ros[a]**

Received (in XXX, XXX) Xth XXXXXXXXX 20XX, Accepted Xth XXXXXXXXX 20XX
DOI: 10.1039/b000000x

Fluorescent bent-core molecules, bearing one or two cyanostilbene units in the lateral structure and different position of the cyano group (α– or β–isomers), are described with the aim to modulate molecular packing and fluorescence properties. These compounds give rise to a variety of crystal polymorphs and bent-core liquid crystalline phases (SmCP, Colr and B6), offering the unique chance to study the fluorescence properties of the cyanostilbene structure in different phases. Experimental and computational studies elucidate geometrical and electronic properties of these bent-core structures but especially the fluorescence properties (spectral positions, quantum yields and decay curves) in a detailed comparison between diluted solutions, in dichloromethane (DCM) or poly(methylmethacrylate) (PMMA), and condensed phases. Quantum yields as high as 70% have been obtained in some diluted solutions (PMMA) and condensed phases. Remarkably, the quantum yield values depend on the position of the cyano group, being higher for β– than for the α–isomers due to higher radiative rates and lower non-radiative rates of the former. The photophysical characterization in the condensed phase focuses on RT studies with solid samples with different processing, and show that, upon aggregation, interactions between the cyanostilbene groups result in changes of the emission spectra and dynamics compared to the diluted systems in DCM and PMMA, giving rise to H-aggregation of varying strength. Furthermore, the compounds exhibit thermochromism, showing a green-yellow fluorescence in the pristine crystalline phase that change to blue on heating to the liquid crystal phase.

Introduction

The cyanostilbene platform has evolved to chromophores of great interest to develop novel functional materials based on low-molecular weight π-conjugated molecules due to their luminescence and electronic characteristics.[1,2] It belongs to the class of fluorophores that is low emissive in liquid solution, but becomes emissive in the solid state, e.g. in solid solution, upon cooling, or aggregation.[3,4] This is mainly due to the suppression of the non-radiative decay channel through restriction of torsional motions,[4] but might be additionally enhanced by appropriate intermolecular arrangement (J-aggregation); this synergetic effect is usually termed aggregation induced enhanced emission (AIEE).[1,5,6] Furthermore, the photophysical properties of cyanostilbenes can be tuned in response to a variety of external stimuli such as heat, pressure, solvents, pH, etc.[7-10]

Several types of functional materials containing cyanostilbenes have been prepared, being nanoparticles,[4,5,11-13] nanowires or nanofibres,[14-18] organogels,[19-24] monolayers,[25] quantum dots,[26] single crystals,[7,27-38] polycrystalline films,[3,7,39-41] etc. In the case of materials with crystalline polymorphism they can exhibit thermochromic properties.[7,42] Relevant relationships between molecular structure, assembly and optical properties have been carefully reviewed recently.[6]

In addition, a few examples of liquid crystalline cyanostilbenes have been reported. The liquid crystal phase opens further possibilities to crystalline materials due to the combination of fluidity and several degrees of packing order. Intrinsic liquid crystalline cyanostilbenes with mesophases like columnar,[43,44] nematic[39,45-51] or smectic phases[39,52,53] have been described. These materials have lead to other interesting phenomena such as fluorescence switching,[39,43,53] photoisomerization-induced phase transition and surface relief gratings.[44] In recent times it has been also shown that incorporation into liquid crystal matrices give rise to photoisomerization-induced phase separation.[54]

In a previous work we have demonstrated that the cyanostilbene unit can also be incorporated in a bent-shaped structure leading to bent-core mesophases.[55] Bent-core liquid crystals (BCLC)[56-68] are a class of non-conventional liquid crystalline phases discovered in 1996[56] that have received significant attention in the soft matter area. Due to their molecular shape they give rise to compact packing that have allowed the development of novel mesophases with polar,

and in some cases, chiral organizations providing so far materials with very attractive functional properties[69-71] such as ferro- and antiferroelectric switching,[57-68] piezoelectric[72,73] or nonlinear optical responses[74-80] from its molecular non-centrosymetric order, but interestingly using achiral molecules. In our case, bent-shaped cyanostilbenes forming columnar mesophases (Col_r) or the polar smectic C mesophase (SmCP), including a dark conglomerate phase (DC-SmCP), have been obtained, with an antiferroelectric ground state in the lamellar phases.[55]

The objective of this work is to study the luminescent properties of these materials in order to obtain novel functional materials characterized by the incorporation of the cyanostilbene unit into a bent-core structure, and to establish relationship between their molecular and supramolecular structures and their optical properties. Herein we report studies carried out for several bent-core molecules bearing one or two cyanostilbene units and with different position of the cyano substituent (named α- or β-families) (Figure 1). The four previously described[55] bent-core compounds bearing two *n*-tetradecyloxy terminal chains, α–B, α,α-B, β-B and β, β-B, and two β-family analogues showing *n*-butoxy terminal chains on the cyanostilbene-containing lateral part, only one for β–BC_4 and two for β,β–BC_4. These two new compounds have been prepared and studied with the aim to modulate molecular packing of bent-shaped molecules by using shorter terminal chains. Our joint experimental and computational studies elucidate geometrical and electronic properties of the bent-core structures, but especially their fluorescence properties, i.e. spectral positions, quantum yields and decay curves, in a detailed comparison between diluted solution and condensed phases, *inter alia* as a function of temperature. Such thermochromism was reported earlier for (liquid) crystalline cyanostilbene compounds,[42,43] however here novelly reported for the structurally more demanding bent-core structures.

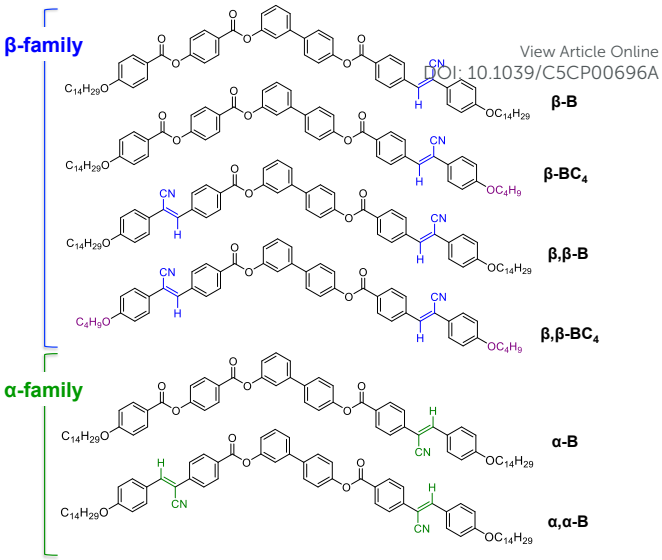

Figure 1. Chemical structures of the cyanostilbene-containing bent-core compounds studied in this work.

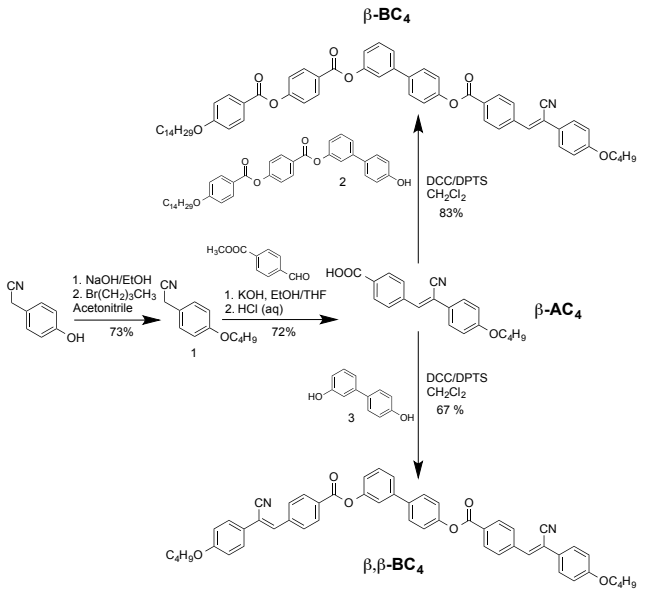

Scheme 1 Synthesis of the *n*-butoxy compounds β-BC_4 and β,β-BC_4.

Results and discussion

Synthesis and structural characterization of β–BC_4 and β,β–BC_4.

Details on the synthesis of bent-core compounds bearing two *n*-tetradecyloxy terminal chains, α-B, α,α-B, β-B and β, β-B were reported in a previous paper.[55] The novel analogues of the β-family, β-BC_4 bearing different terminal chains and β,β-BC_4 with two *n*-butoxy terminal chains have been prepared according to the synthetic pathways shown in Scheme 1. In the last step of the synthetic route either a single or double esterification reaction of the acid β-AC_4 with compound 2 or 3 occurs, using dicyclohexylcarbodiimide (DCC) and 4-(dimethylamino)pyridinium *p*-toluenesulfonate (DPTS), giving the final compounds in high yields. Experimental details and their characterization data from NMR, FTIR, MS and elemental analysis are collected in the ESI.

Thermal and liquid crystal properties of the compounds.

Phase transitions of the *n*-butoxy bent-core compounds β-BC_4 and β,β-BC_4 were studied by polarizing optical microscopy (POM) and differential scanning calorimetry (DSC). Results are shown in Table 1. Liquid crystalline properties of the previously reported *n*-tetradecyloxy bent-core cyanostilbenes[55] have been also enclosed in Table 1 for comparison.

All compounds exhibit complex solid polymorphism. The DSC thermograms show that in all cases the solid phase obtained at RT after a heating/cooling cycle at 10 ºC min^{-1} is

different from the initial crystal phase (pristine powder) then, the second heating cycle is different from the first one. That is why in Table 1 the first heating-cooling cycle, and the second heating cycle are shown. In addition, complex crystal-to crystal transitions are observed before the liquid crystal phase appears.

Due to the complexity of these processes the Table 1 collects a simplified version of the crystal transitions, where Cr represents any crystal phase, and detailed information about the crystal polymorphism are displayed in the DSC thermograms collected in the ESI (Figures S2, S3) and in ref 55. The cooling cycles, on the other hand, are always reproducible.

In general, compounds with two cyanostilbene groups have higher melting points that the ones with only one cyanostilbene group.

Compounds with two terminal *n*-tetradecyloxy chains are all liquid crystals. β-B, β,β-B and α-B show lamellar type phases ($SmCP_A$) with antiferroelectric polar switching, and α-B and α,α-B, show columnar phases (Col_r)[55] (Figure 2).

The new compounds with shorter *n*-butoxy tails, β-BC_4 and β,β-BC_4, give both higher melting points and different liquid crystalline packing compared to the corresponding *n*-tetradecyloxy analogues.

Table 1 Thermal transisions of the bent-core cyanostilbenes

Compound	Phase transition (T / ºC) [ΔH / kJ mol-1] [a, b]
β-BC_4	Cr 128 (44.0)[c] Col_r 156 (16.2) I I 153 (15.0) Col_r 72 (27.0) Cr Cr 125 (40.1) Col_r 157 (15.4) I
β,β-BC_4	Cr 186 (22.1)[c] M 196 (8.2) I I 193 (8.7) M 86 (9.7) Cr Cr 194 M 196 (39.4)[c] I
β-B[55]	Cr 93 (61.3) $SmCP_A$ 167 (23.7) I I 164 (23.2) $SmCP_A$ 45 (15.9) Cr Cr 90 (39.1) $SmCP_A$ 166 (23.4) I
β,β-B[55]	Cr 134 (46.7)[c] $SmCP_A$ 177 (23.2) I I 174 (22.1) DC 106 (55.5) Cr Cr 133 (49.8)[c] $SmCP_A$ 177 (22.2) I
α-B[55]	Cr 89 (53.3)[c] $SmCP_A$ 148[d] Col_r 164 (18.1) I I 160 (18.1) Col_r 115[d] $SmCP_A$ 33 (8.7) Cr Cr 86 (2.6) $SmCP_A$ 148[d] Col_r 163 (16.7) I
α,α-B[55]	Cr 134 (58.3) Col_r 191 (20.3) I I 188 (20.0) Col_r 89 (87.2) Cr Cr 107 (88.8)[c] X[e] 132 (0.7) Col_r 190 (19.9) I

[a] Data determined by DSC, showing first heating and cooling cycles, and second heating cycle at a scanning rate of 10 ºC min^{-1} (maximum of the peaks). Cr: crystal, $SmCP_A$: antiferroelectric polar smectic C mesophase, DC: dark conglomerate mesophase, Col_r: rectangular columnar mesophase, M: unidentified mesophase, tentatively assigned as B_6, [b] The crystal phase denoted as Cr is, in most cases, not unique and crystalline polymorphism with complex transitions appear (see thermograms in the ESI), [c] Combined enthalpy of several crystalline transitions; [d] Data obtained from dielectric spectroscopy. [e] Depends on the thermal history, at 10 ºC min^{-1} is an unstable SmCP mesophase which recrystallizes to Cr on heating.

Compound β-BC_4 displays a *pseudo* focal-conic and mosaic texture in the POM image (Figure 3a), consistent with a columnar mesophase.[69,81] X-ray diffractograms show two reflections in the small angle region corresponding to distances of 32.9 and 23.5 Å, that exclude a hexagonal columnar mesophase, but compatible with a rectangular columnar mesophase (Col_r) (Figure 2). Compound β,β-BC_4 shows a fan-shaped texture upon cooling (Figure 3b) without homeotropic regions or Schlieren textures when shearing the sample. This behavior has been reported for B_6-type intercalated smectic phases, which are lamellar phases in which the molecules are interdigitated (Figure 2).[82] However, in this case it could not be confirmed by X-ray diffraction for β,β-BC_4 due to the metastable character of this mesophase (abbreviated as M in Table 1), which crystallizes during data collection, precluding its conclusive identification.

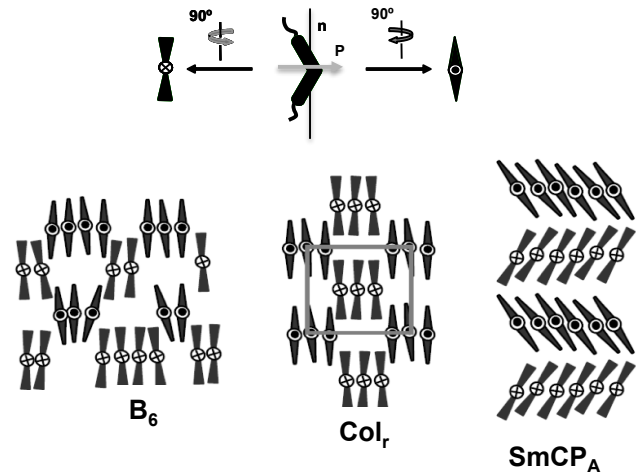

Figure 2. Schematic representations of a bent-shaped molecule, and organization of the molecules in the bent-core mesophases proposed for the compounds studied in this work: B_6, Col_r and $SmCP_A$ packings.

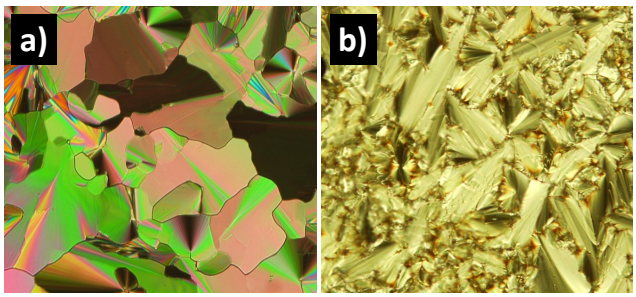

Figure 3. Photomicrographs between crossed polarizers of a) columnar phase texture at 150 °C for compound β-BC_4, and b) fan-shaped texture at 188 °C for compound β,β-BC_4 consistent with a B_6 mesophase.

It has been reported that, as a general trend, the ratio between flexible and rigid structures, i.e. between terminal chains and aromatic cores, affects the microsegregation of these parts of the molecules and hence the supramolecular arrangements achieved.[83] Shorter terminal chains give rise to intercalation of the molecules, generating B_6 or nematic

phases. On increasing the number of carbons in the chain, the balance between the two moieties of the molecule precludes intercalation, giving rise to an organization in ribbons, and thus leading to Col_r phases, which usually do not show any response to an electric field. Results of these two new *n*-butoxy bent-core compounds agree with these expectations.

The bent-core mesophases are promoted by the neat bent-shaped geometry of the compounds. According to density functional theory (DFT) applied for methoxy-analogs, both α–B and β-B molecules show significant twisting of the backbone (Figure 4), in particular within the biphenyl unit (torsional angle θ_1 = 40 º) and in the cyanovinylene unit where the phenyl rings in direct proximity to the cyano group are strongly tilted (θ_2 = 29 º for α-B and θ_2 = 31 º for β-B). However, substantial planarization of the backbones in the mesophases might occur, promoted by the twist elasticity of the cyanostilbene motif.[1,2] Here, the local dipoles of the cyano-groups are expected to drive the molecules into a parallel arrangement with the cyano-groups in a slip-stack fashion.[6]

On the other hand, taking into account the strong tendency for 3,4´-biphenyl-compounds to promote lamellar organization in mesophase (SmCP) for long terminal tails, differences on the polar cyano-group orientation in the α– and β-compounds, shown by the optimized geometries (Figure 4), could be in the origin for the different liquid crystal behavior found, tending to columnar-type mesophases for the α-B, and α,α-B. In addition, as we mentioned above, all these bent-shaped cyanostilbenes exhibit an outstanding solid polymorphism that can be revealed by thermal treatments of pristine samples. Furthermore, when two long terminal tails are present, glassy mesophase-like organizations can be achieved on fast cooling from the mesophase and detected by POM and XRD at room temperature. Interestingly, many of these molecular aggregations visually offer fluorescence differences.

Photophysics in solution.

The UV-Vis spectra in dichloromethane (DCM) solution of these compounds exhibit two distinct absorption bands, one around 353-358 nm (A_1 band) and one around 266 nm (A_2 band) (Figure 5), with varying intensities within the family of compounds, see Table 2. According to our time-dependent (TD) DFT calculations (for details see the ESI), A_1 of α-B and β-B essentially contains the first two singlet electronic excitations. $S_0 \rightarrow S_1$ is mainly formed from the frontier MOs (HOMO→LUMO) located on the cyanostilbene unit, whereas $S_0 \rightarrow S_2$ exhibits strong charge-transfer (CT) character arising mainly from a HOMO-1→LUMO excitation, where HOMO-1 is located on the biphenyl core. In the α,α- and β,β-compounds, the A_1 band exhibits roughly double intensity compared to the α-/β-compounds due to the presence of two cyanostilbene units. The A_2 band, on the other hand, is mainly formed by biphenyl-centered and phenyl benzoate centered transitions.

All cyanostilbene compounds emit around 450 nm; however, the quantum yields are low in general, in agreement with those reported in literature.[3,4] This was described earlier to the slow excited state planarization which opens an effective channel towards a conical intersection for internal conversion to the ground state via torsional modes.[4] The latter are effectively hindered in solid environments. To test this we prepared highly diluted PMMA films, where the molecules are still molecularly dissolved, however in a rigid environment; in fact, in PMMA the compounds showed significant enhancement of fluorescence (Table 2).

Table 2. UV-Vis and fluorescence data in dichloromethane (DCM) solution and dissolved in PMMA: Absorption and emission maxima (λ_{abs}, λ_{em}), fluorescence quantum yields (Φ_F), and lifetimes (τ_F), radiative and non-radiative rates (k_r, k_{nr}).

	DCM				PMMA				
	λ_{abs} / nm	ε_m / 10^4 L mol^{-1} cm^{-1}	λ_{em} / nm	Φ_F [a]	λ_{em} / nm	Φ_F [b]	τ_F [c] / ns	k_r [d] / s^{-1}	k_{nr} [d] / s^{-1}
β-BC_4	A2: 267 A1: 354	5.6 3.2	450	0.09	423	0.55	1.66	$3.3 \cdot 10^8$	$2.7 \cdot 10^8$
β,β-BC_4	A2: 264 A1: 354	3.3 6.0	450	0.09	426	0.61	1.65	$3.7 \cdot 10^8$	$2.4 \cdot 10^8$
β-B	A2: 267 A1: 354	5.5 3.1	450	0.08	422	0.55	1.60	$3.4 \cdot 10^8$	$2.8 \cdot 10^8$
β,β-B	A2: 264 A1: 353	3.4 6.0	450	0.08	427	0.62	1.56	$4.0 \cdot 10^8$	$2.4 \cdot 10^8$
α-B	A2: 267 A1: 356	4.0 3.3	442	< 0.001	422	0.01	0.70	$1.4 \cdot 10^7$	$1.4 \cdot 10^9$
α,α-B	A2: 267 A1: 358	3.0 7.8	442	< 0.001	431	0.01	0.46	$2.2 \cdot 10^7$	$2.2 \cdot 10^9$

[a] From relative measurements using 9,10-diphenylanthracene in cyclohexane as reference (Φ_F = 0.9). [b] From absolute measurements in an integrating sphere. [c] Intensity averages from bi-exponential fits (see ESI). [d] From $\tau_F = 1/(k_r + k_{nr})$, $\Phi_F = k_r \cdot \tau_F$.

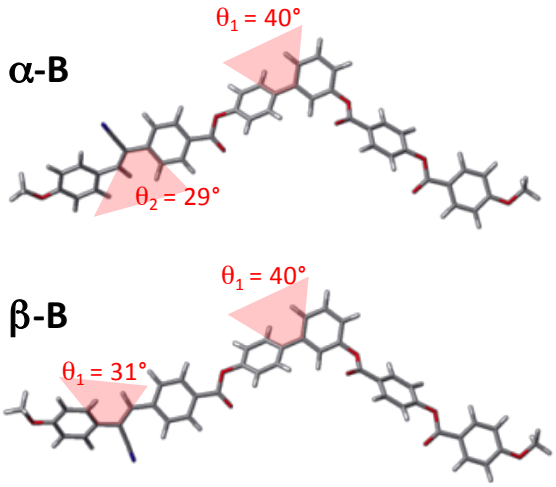

Figure 4. Optimized geometries of α-B and β-B bent-core molecules with methoxy-terminal tails.

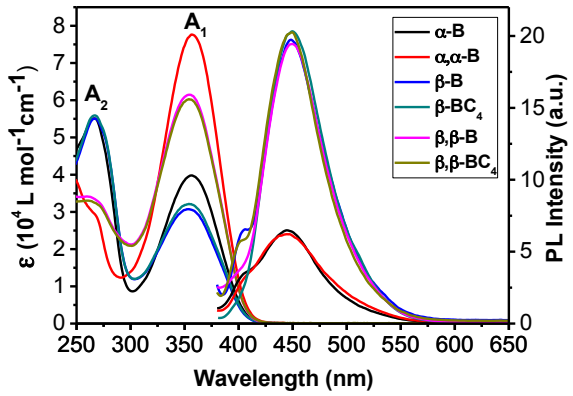

Figure 5. Absorption and fluorescence spectra of bent-core compounds in dichloromethane solutions (A_i, see Table 2). The original fluorescence spectra have been divided by the absorbance at the excitation wavelength for better comparison. For α-compounds, the fluorescence spectra were multiplied by 100.

Remarkably, the quantum yield values are quite different depending on the position of the cyano-group, being below 0.001 for the α-family and in the range of 0.07-0.09 for the β–family in DCM, and also in PMMA the differences are still significant (0.01 vs. 0.60). Extraction of the radiative and non-radiative rates (k_r, k_{nr}, see Table 2) demonstrates significantly lower radiative rates for the α-compared to the β-family, and at the same time much higher non-radiative rates for the α-family, pointing to the fact that torsional relaxation depends sensitively on structural factors and influences both radiative and non-radiative decay channels.[83] These findings will be discussed in more detail in a forthcoming report.[85] Interestingly, the fluorescence spectra in PMMA all exhibit a significant blue shift against DCM. This cannot be due to a polarizability effect, since the latter is higher in PMMA. We thus rather ascribe this effect to a freezing out of non-planar excited state conformations in PMMA,[85] whereas in DCM broad conformational distributions are expected.[86]

Photophysics in the Solid Phases.

The photophysics of all compounds were investigated in the bulk, i.e. in the solid polymorphs and mesophases, in order to understand aggregation effects in detail. It should be noted that the liquid crystalline samples (high temperature) show photoinstability during the laser irradiation through a combination of laser intensity, temperature and fluidity, preventing experiments at high temperatures. Thus, the photophysical characterization was focused on room temperature (RT) studies with different solid samples (Table 3): the as-obtained solid (identified as *pristine*), and processed solids, i.e. films cooled down from the mesophase at 10 °C min^{-1} and remaining at RT for one day (identified as slow cooled film, *scf*). In addition, for the *n*-tetradecyloxy compounds β–B, β,β–B, α-B and α,α-B, films were also prepared by fast cooling (0 °C quenching) from the mesophase (identified as fast cooled film, *fcf* in Table 3); here, XRD confirmed that this method allows to freeze the organization of the liquid crystal phase at RT.

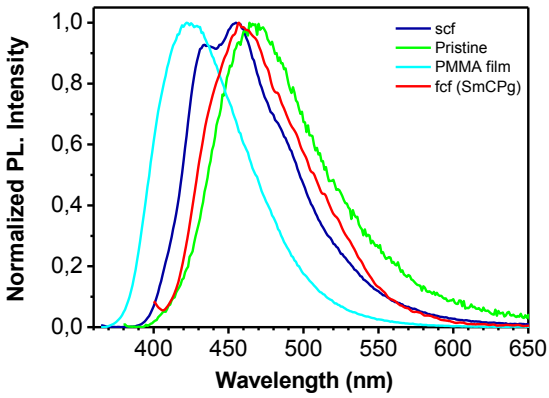

Figure 6. Fluorescence spectra of β-B in different solid samples. Pristine powder (green), scf: slow cooled film at 10 °C min^{-1} (dark blue), fcf; fast cooled film (glassy SmCP) (red), solid solution in PMMA (light blue).

View Article Online
DOI: 10.1039/C5CP00696A

Table 3 Fluorescence data in the condensed phases: Emission maxima (λem), fluorescence quantum yields (Φ_F), and lifetimes (τ_F), radiative and non-radiative rates (k_r, k_{nr}), relative rates against PMMA, assignment of H/J-aggregation, in/decrease of the free volume.

Compound	sample	λ_{em} / nm	Φ_F [a]	$\langle\tau_F\rangle$ [b] / ns	k_r [c] / s^{-1}	k_{nr} [c] / s^{-1}	$k_r/k_{r,PMMA}$	$k_{nr}/k_{nr,PMMA}$	H/J [d]	Free vol. [e]
β-BC4	*pristine* [f]	495	0.72	12.9	$5.6\cdot10^7$	$2.2\cdot10^7$	0.17	0.08	H	--
	scf	478	0.27	5.9	$4.5\cdot10^7$	$1.2\cdot10^8$	0.14	0.44	H	-
β,β-BC_4	*pristine*	476	0.35	6.47	$5.4\cdot10^7$	$1.0\cdot10^8$	0.15	0.42	H	-
	scf	475	0.63	3.97	$1.6\cdot10^8$	$9.3\cdot10^7$	0.43	0.39	wH	-
β-B	*pristine*	468	0.03	1.43	$2.1\cdot10^7$	$6.8\cdot10^8$	0.06	2.43	H	+
	scf	455	0.24	1.25	$1.9\cdot10^8$	$6.1\cdot10^8$	0.56	2.18	wH	+
	fcf ($SmCP_g$)	457	0.04	3.43	$1.2\cdot10^7$	$2.8\cdot10^8$	0.04	1.00	H	+/-
β,β-B	*pristine*	493	0.04	3.71	$1.1\cdot10^7$	$2.6\cdot10^8$	0.03	1.08	H	+/-
	scf	470	0.15	1.90	$7.9\cdot10^7$	$4.5\cdot10^8$	0.20	1.88	H	+
	fcf (*DC-SmCP*$_g$)	478	0.12	3.33	$3.6\cdot10^7$	$2.6\cdot10^8$	0.09	1.08	H	+/-
α-B	*pristine*	497	0.03	2.80	$1.1\cdot10^7$	$3.5\cdot10^8$	0.79	0.25	H	-
	scf	476	0.01	0.47	$2.1\cdot10^7$	$2.1\cdot10^9$	1.50	1.50	H/J	+
	fcf ($SmCP_g$)	471	0.01	1.06	$9.4\cdot10^6$	$9.3\cdot10^8$	0.67	0.66	wH	+/-
α,α-B	*pristine*	495	0.01	0.68	$1.5\cdot10^7$	$1.5\cdot10^9$	0.68	0.68	wH	+/-
	scf	494	0.02	1.84	$1.1\cdot10^7$	$5.3\cdot10^8$	0.50	0.24	wH	-
	fcf (Col_{rg})	494	0.01	1.30	$7.7\cdot10^6$	$7.6\cdot10^8$	0.35	0.35	H	-

[a] from absolute measurements in an integrating sphere. [b] intensity averages from tri-exponential fits (see SI). [c] from $\tau_F = 1/(k_r + k_{nr})$, $\Phi_F = k_r \cdot \tau_F$. [d] H/J-aggregation assignment from comparison of k_r to PMMA. [e] in-/decrease of free Volume from comparison of k_{nr} to PMMA. [f] *pristine*: powder as-obtained solid sample, *scf*: film from processed solid by slow cooling at 10 ºC/min, *fcf*: film from processed solid by fast cooling from mesophase (0 ºC quenching); $SmCP_g$: vitrified SmCP mesophase; Col_{rg}: vitrified Col_r mesophase.

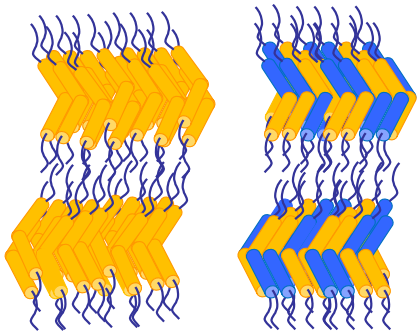

Figure 7. Schematic representations of general packing models for compounds with two cyanostilbene units (left) and one cyanostilbene unit (right) in the condensed phases, where H-aggregation of the cyanostilbene-containing lateral part (in orange color) is shown.

Upon aggregation, interactions between the chromophores result in (partly) significant changes of the emission spectra and dynamics compared to the diluted systems in DCM and PMMA (Table 3). The main contribution arises from molecular excitons formed by interaction of the molecular $S_0 \rightarrow S_1$ transition dipoles moments (TDM), which in case of 'side-by-side' ('head-to-tail') orientation lead to H- (J-) aggregation[87,88,89] with blue (red-) shifted absorption spectra, and smaller (larger) radiative rates compared to solution. Since there is often confusion in literature, it should be noted that since Kasha's original model based on point dipoles[87] is not suitable for closely packed aggregates, quantum-chemical models have to be used instead.[6] It should also be reminded that the molecular exciton model only tells something about energies and oscillator strengths (and thus radiative rates) of exciton states, but not on efficiencies (Φ_F),[84] since the latter not only depend on k_r but also non-radiative rates k_{nr}. Finally, for samples with higher optical densities (powders and thicker films), assignment of H/J-aggregation cannot rely on spectral shifts,[84] but rather on radiative rates.[6]

The emission spectra of the condensed phases are red-shifted against (solid) solution, see Figure 6 and Table 3. This is partly due to excitonic effects, but also due to the higher (anisotropic) polarizability compared to solution.[90] The radiative rates are all smaller than in PMMA (with exception of α-B *scf*), indicating H-aggregation, however with varying degree (Table 3). In the *scf* phase of α-B, a 50% enhancement of k_r against PMMA is observed, which we however mainly ascribe to the higher polarizability in the condensed phase since k_r scales with the square of the refractive index[91,92] so that excitonic effects are very small in this sample. H-aggregation can be rationalized by the common 'bent-core bunch' packing features of these bent-shaped structures, in which the TDM of neighboring cyanostilbenes (being oriented along the conjugated core), will be only slightly shifted against each other (Figure 7). Anyway, packing can vary significantly for these compounds, and depending on the preparation method (as-obtained solid vs. processed solids from heated samples), different degrees of H-aggregation are obtained; fast cooling might further freeze out different arrangements, e.g. keeping a similar packing to the liquid crystal phase ($SmCP_A$ or

Col_r), depending on the compound (Table 3). Specifically, strong H-aggregation was observed for β-B and β,β-B in the SmCP and pristine phases, respectively. However, it's difficult to make more far-reaching conclusions, due to the strong dependency on preparation history. In particular, for many of the compounds the crystal phase obtained in the first cooling is not stable and evolves with time to different ones, which are not identical to the former.

The different solid-state arrangements give rise to varying degrees of free volume as can be qualitative deduced from the change of the non-radiative rates against (solid) solution, since dense packing gives rise to small free volume, and thus low internal conversion rates. Here, a significant smaller free volume is observed for compounds with short terminal tails compared to those with two long *n*-tetradecyloxy chais (Table 3). Thus, highly luminescent bent-core cyanostilbene materials should combine large molecular k_r with weak H-aggregation and low free volume, which in fact gives a hierarchy of luminescence in the order α-/α,α-B ≈ β-B < β,β-B << β-/β,β-BC_4.

Thermochromism.

As discussed earlier, the bent-core cyanostilbenes give rise to a variety of crystal polymorphs and liquid crystalline phases, offering the unique chance to study the fluorescence properties as a function of temperature. In general all compounds show thermochromism with a blue- shift of the fluorescent wavelength on heating.

We were able to record visual changes of the fluorescence color by taking pictures of films at different temperatures using as excitation source a handheld 365 nm UV lamp during short exposition times. Under these conditions the compounds did not suffer from photoreactions at high temperature. But, using the light source of the spectrometer to excite the samples at high temperature was not reliable due to the lack of stability of the compounds, which prevented to obtain the real fluorescence spectra at variable temperature.

For the α-compounds, which have shown to be low luminescent in the pristine powder at room temperature (vide supra), the luminescence in the liquid crystal phases on heating was barely visible. For the β-compounds, as they show higher luminescent quantum yields in the pristine solid compared to the α-compounds, the thermochromism becomes more evident, as demonstrated for compound β-BC_4 in Figure 8. For β-BC_4, the pristine powder (Cr_1) show a yellow-green luminescence and undergoes a blue-shift on heating to the liquid crystal phase (Col_r), and a further blue-shift on passing to the isotropic liquid (I). Upon cooling from the isotropic liquid to room temperature, the luminescence intensity increases while the spectra are red-shifted. The wavelength emission of the crystal phase obtained from cooling (Cr_2) is different from the pristine solid (Cr_1). This crystalline phase (Cr_2) however is not stable and transforms, after one day, to another polymorph (*scf* in Table 3) that is more luminescent and with a red-shifted emission. This change does not bear any apparent clear change at the DSC. The significant changes in the fluorescence color demonstrate that it is very sensitive to small environmental changes.

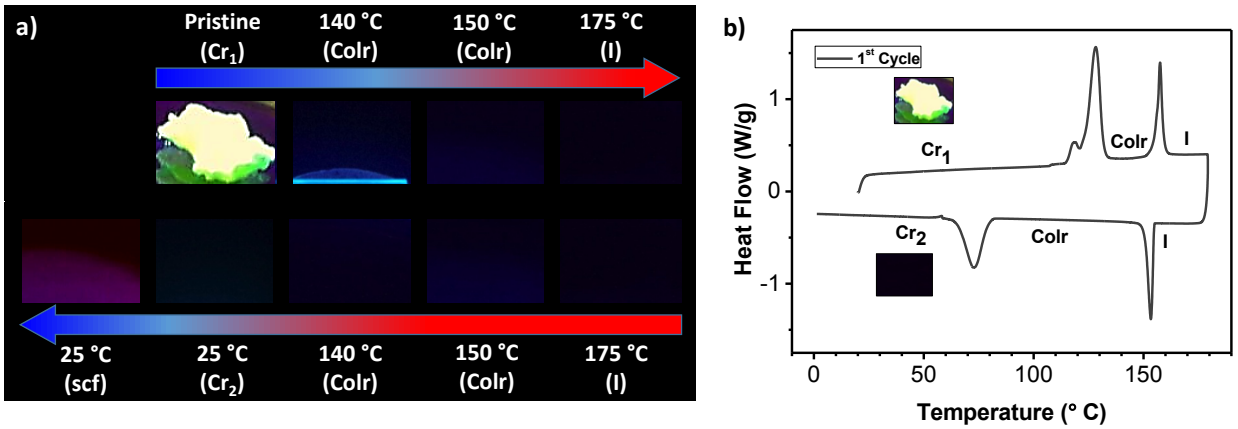

Figure 8. a) Thermochromism of β-BC_4; b) first cycle DSC thermogram (10 °C min^{-1}) of β-BC_4 with the photographs under UV light of the as-obtained solid (Cr_1 or pristine) and the crystal phase (Cr_2) obtained from cooling at RT.

Experimental

Materials and methods.

Chemical reagents used in this study were purchased from Aldrich and were used without further purification. ^{1}H-NMR spectra were recorded on spectrometers operating at 300.13 MHz (ARX-300 and AV-300) and 400.17 MHz (AV-400), whereas ^{13}C-NMR spectra were recorded at 75.47 MHz and 100.62 MHz, respectively, on the same spectrometers. The compositions of the synthesized compounds were determined by elemental analysis performed on a Perkin-Elmer 240C CHNS elemental analyzer. FT-IR spectra were performed in a ThermoNicolet Avatar 360 using KBr pellets. Mass spectral data (MALDI+) were obtained using a Microflex (MALDI-ToF). The preliminary mesophase identification was based on microscopic examination of the textures formed by samples between two glass plates. Nikon and Olympus BH-2 polarizing microscopes equipped with a Linkam THMS600 hot stage were used. The temperatures and enthalpies of the phase transitions were determined by calorimetric measurements with DSC TA Instrument Q-20 system. Molecular dimensions were estimated by molecular modeling (ChemSketch3D). The X-ray investigations on non-oriented samples were carried out in Lindemann capillary tubes (diameter 0.9 mm) using a Pinhole (Anton-Paar) film camera. Synthetic procedures and characterization data of the novel compounds are reported in the ESI.

Solid solutions of cyanostilbene molecules were prepared by adding a solution of cyanostilbene bent core molecules to a solution of PMMA in dichloromethane and stirred to have a homogeneous mixture. The concentration of the molecules were kept below 0.01 (w/w)%. The solution was then spin coated on a fused silica substrate to form a solid solution of these molecules in the PMMA matrix.

Photophysical Measurements.

Absorption and fluorescence measurements in solution were carried out using ATI-Unicam UV4-200 and PERKIN-ELMER LS50B instrument, respectively. Fluorescence emission in solid state was measured in Horiba FluoroLog 3 Spectrophotometer, equipped with double monochromators at the emission and excitation sides. Fluorescence lifetime experiments were performed by the time-correlated single photon counting (TCSPC) technique. The excitation source was a 405 nm picosecond pulsed diode laser (LDH-D-C-405, PicoQuant) driven by a PDL828 driver (PicoQuant) with FWHM < 70ps. The emission was dispersed in wavelength using an Acton SP2500 spectrometer (as mentioned above) and detected by a blue sensitive, low dark current photomultiplier (PMA 06, PicoQuant), which covers a spectral range from 220 to 650 nm (transit time spread < 50 ps, FWHM). A HydraHarp-400 TCSPC event timer with 1 ps time resolution was used to measure the fluorescence decays. The PL quantum efficiencies of solutions and in condensed phases were measured in an absolute quantum yield measurement system (Hamamatsu, C9920) with a detection range from 300 nm to 950 nm and bandwidth from 2 nm to 5 nm (FWHM).

Quantum-chemical Calculations.

The geometries were optimized without symmetry restriction at the density functional theory (DFT) level, employing the B3LYP functional and the 6-311G* basis set as implemented in the Gaussian09 program package.[93] Vertical excited states of anti and syn rotamers were calculated using time-dependent (TD)DFT (B3LYP/6-311G*).

Summary and Conclusions

Novel fluorescent bent-core molecules containing the high current interest cyanostilbene structure have been prepared and characterized. It is shown that molecular packing of these bent-shaped cyanostilbenes can be modulated by the number of chromophores (one or two cyanostilbene units), the position of the cyano-group (α– or β–families) and the length of the terminal alkoxy chains. Indeed, rich crystal polymorphism and bent-core liquid crystal phases (SmCP, Col_r and B_6 mesophases) have been obtained.

Fluorescent properties are different in diluted liquid solution (DCM), diluted solid solution (PMMA) and condensed phases. The increase in quantum yield and the blue shift of the emission maxima in PMMA (around 420 nm) with respect to DCM (around 450 nm) is ascribed to a freezing out of non-planar excited state conformations in PMMA, whereas in DCM broad conformational distributions are expected. Remarkably, the quantum yield values are also different depending on the position of the cyano-group, being below 0.001 for the α-family and in the range of 0.07-0.09 for the β–family in DCM, and also in PMMA the differences are still significant (0.01 vs. 0.60). Studies in solid samples at RT show that upon aggregation, interactions between the chromophores result in changes of the emission spectra and dynamics compared to the diluted systems in DCM and PMMA. The radiative rates are all smaller than in PMMA, indicating H-aggregation for almost all compounds with varying degree depending on the packing, which is rationalized by the common "bent-core bunch" packing features of these bent-shaped structures. Short-chain compounds, β–BC_4 and β,β–BC_4, are specially interesting as crystal phases with very high quantum yields (up to 0.7) have been obtained, and combine large molecular radiative rates, weak H-aggregation and low free volume.

Finally, thermochromic properties have been described with significant changes (from yellow-green to blue) in fluorescence measured in the different phases on heating or cooling.

In conclusion, these compounds show that the incorporation of the cyanostilbene unit in a bent-core liquid crystal-type structure gives rise to a rich phenomenology in terms of molecular structure and packing arrangements, which translates in changes in the fluorescent properties, giving rise to systems that are very sensitive to small environmental changes.

Acknowledgements

The authors from ICMA greatly appreciate financial support from the Spanish Government (MINECO-FEDER project MAT2012-38538-C03-01), the Aragon's Government and FSE (project E04) and the JAE.PREDOC-CSIC (M. M-A) fellowship program. Thanks are given also to Nuclear Magnetic Resonance, Mass Spectra and Thermal Analysis Services from the Instituto de Ciencia de Materiales de Aragón (Uni. Zaragoza–CSIC).

The work at IMDEA was supported by the Spanish Government (MINECO-FEDER project CTQ2011-27317), by the Comunidad de Madrid (Project S2009/MAT-1726, S2009/PPQ-1533) and by the Campus of International Excellence (CEI) UAM+CSIC. We thank H. Bolink, Valencia, for access to the integrating sphere.

Notes and references

[a] *Instituto de Ciencias Materiales de Aragón (ICMA), Universidad de Zaragoza-CSIC, Departamento de Química Orgánica, Facultad de Ciencias, 50009, Zaragoza, Spain*
[b] *Instituto Madrileño de Estudios Avanzados en Nanociencia (IMDEA Nanociencia), Ciudad Universitaria de Cantoblanco, E-28049, Madrid, Spain*
[c] *current address: School of Physics and Astronomy, University of St Andrews, UK*
[d] *Departamento de Química Física, Facultad de Química, Universidad de Valencia, Spain*

† Electronic Supplementary Information (ESI) available: [Synthesis, NMR spectra and DSC thermograms of compounds β-BC_4 and β,β-BC_4. Additional photophysical data and quantum chemical calculations]. See DOI: 10.1039/b000000x/

1 B.-K. An, J. Gierschner and S. Y. Park, *Acc. Chem. Res.*, 2012, **45,** 544-554.
2 L. Zhu and Y. Zhao, *J. Mater. Chem. C*, 2013, **1,** 1059-1065.
3 D. Oelkrug, A. Tompert, H. J. Egelhaaf, M. Hanack, E. Steinhuber, M. Hohloch, H. Meier and U. Stalmach, *Synth. Met.*, 1996, **83**, 231-237.
4 D. Oelkrug, A. Tompert, J. Gierschner, H. J. Egelhaaf, M. Hanack, M. Hohloch and E. Steinhuber, *J. Phys. Chem. B*, 1998, **102**, 1902-1907.
5 B. K. An, S. K. Kwon, S. D. Jung and S. Y. Park, *J. Am. Chem. Soc.*, 2002, **124**, 14410-14415.
6 J. Gierschner and S. Y. Park, *J. Mater. Chem. C*, 2013, **1**, 5818-5832.
7. S.-J. Yoon, J. W. Chung, J. Gierschner, K. S. Kim, M.-G. Choi, D. Kim and S. Y. Park, *J. Am. Chem. Soc.*, 2010, **132**, 13675-13683.
8 M. S. Kwon, J. Gierschner, J. Seo and S. Y. Park, *J. Mater. Chem. C*, 2014, **2**, 2552-2557.
9 Y. Zhang, J. Sun, X. Lv, M. Ouyang, F. Cao, G. Pan, L. Pan, G. Fan, W. Yu, C. He, S. Zheng, F. Zhang, W. Wang and C. Zhang, *Cryst. E ng . Comm.*, 2013, **15**, 8998-9002.
10 Y. Zhang, K. Wang, G. Zhuang, Z. Xie, C. Zhang, F. Cao, G. Pan, H. Chen, B. Zou and Y. Ma, *Chem. Eur. J.*, 2015, **21**, 2474-2479.
11 S.-J. Lim, B.-K. An, S. D. Jung, M.-A. Chung and S. Y. Park, *Angew. Chem. Int. Ed.*, 2004, **43**, 6346-6350.
12 H. Nam, B. Boury and S. Y. Park, *Chem. Mater.*, 2006, **18**, 5716-5721.
13 Y. Zhang, J. Sun, G. Bian, Y. Chen, M. Ouyang, B. Hu and C. Zhang, *Photochem. Photobiol. Sci.*, 2012, **11**, 1414-1421.
14 B. K. An, S. H. Gihm, J. W. Chung, C. R. Park, S. K. Kwon and S. Y. Park, *J. Am. Chem. Soc.*, 2009, **131**, 3950-3957.
15 J. H. Kim, A. Watanabe, J. W. Chung, Y. Jung, B.-K. An, H. Tada and S. Y. Park, *J. Mater. Chem.*, 2010, **20**, 1062-1064.
16 S. W. Yun, J. H. Kim, S. Shin, H. Yang, B.-K. An, L. Yang and S. Y. Park, *Adv. Mater.*, 2012, **24**, 911-915.
17 S. Shin, S. H. Gihm, C. R. Park, S. Kim and S. Y. Park, *Chem. Mater.*, 2013, **25,** 3288-3295.
18 Y. Jin, Y. Xia, S. Wang, L. Yan, Y. Zhou, J. Fan and B. Song, *Soft Matter*, 2015, **11**, 798-805.
19 B. K. An, D. S. Lee, J. S. Lee, Y. S. Park, H. S. Song and S. Y. Park, *J. Am. Chem. Soc.*, 2004, **126**, 10232-10233.
20 J. W. Chung, B. K. An and S. Y. Park, *Chem. Mater.*, 2008, **20**, 6750-6755.
21 S.-J. Yoon, J. H. Kim, J. W. Chung and S. Y. Park, *J. Mater. Chem.*, 2011, **21**, 18971-18973.
22 J. Seo, J. W. Chung, I. Cho and S. Y. Park, *Soft Matter*, 2012, **8,** 7617-7622.
23 Y. Zhang, C. Liang, H. Shang, Y. Ma and S. Jiang, *J. Mater. Chem. C*, 2013, **1**, 4472-4480.
24 J. Seo, J. W. Chung, J. E. Kwon and S. Y. Park, *Chem. Sci.*, 2014, **5**, 4845-4850.
25 A. Gulino, F. Lupo, G. G. Condorelli, M. E. Fragalà, M. E. Amato and G. Scarlata, *J. Mater. Chem.*, 2008, **18**, 5011-5018.
26 L. Zhu, C. Y. Ang, X. Li, K. T. Nguyen, S. Y. Tan, H. Ågren and Y. Zhao, *Adv. Mater.*, 2012, **24**, 4020-4024.
27 W. Xie, Y. Li, F. Li, F. Shen and Y. Ma, *Appl. Phys. Lett.*, 2007, **90**, 141110.
28 Y. Li, F. Shen, H. Wang, F. He, Z. Xie, H. Zhang, Z. Wang, L. Liu, F. Li, M. Hanif, L. Ye and Y. Ma, *Chem. Mater.*, 2008, **20,** 7312-7318.
29 H. Wang, F. Li, I. Ravia, B. Gao, Y. Li, V. Medvedev, H. Sun, N. Tessler and Y. Ma, *Adv. Funct. Mater.*, 2011, **21**, 3770-3777.
30 S. J. Yoon and S. Park, *J. Mater. Chem.*, 2011, **21**, 8338-8346.
31 X. Li, Y. Xu, F. Li and Y. Ma, *Org. Electron.*, 2012, **13**, 762-766.
32 S. Varghese, S. J. Yoon, E. M. Calzado, S. Casado, P. G. Boj, M. A. Díaz-García, R. Resel, R. Fischer, B. Milián-Medina, R. Wannemacher, S. Y. Park and J. Gierschner, *Adv. Mater.*, 2012, **24**, 6473-6478.
33 Y. Xu, H. Zhang, F. Li, F. Shen, H. Wang, X. Li, Y. Yu and Y. Ma, *J. Mater. Chem.*, 2012, **22**, 1592-1597.

34 S. K. Park, S. Varghese, J. H. Kim, S.-J. Yoon, O. K. Kwon, B.-K. An, J. Gierschner and S. Y. Park, *J. Am. Chem. Soc.*, 2013, **135**, 4757-4764.

35 S. Varghese, S. K. Park, S. Casado, R. C. Fischer, R. Resel, B. Milián-Medina, R. Wannemacher, S. Y. Park and J. Gierschner, *J. Phys. Chem. Lett.*, 2013**, 4**, 1597-1602.

36 S. J. Yoon, S. Varghese, S. K. Park, R. Wannemacher, J. Gierschner and S. Y. Park, *Adv. Opt. Mat.*, 2013, **1**, 232-237.

37 Y. Li, F. Li, H. Zhang, Z. Xie, W. Xie, H. Xu, B. Li, F. Shen, L. Ye, M. Hanif, D. Ma and Y. Ma, *Chem. Commun.*, 2007, 231-233.

38 H.-H. Fang, Q.-D. Chen, J. Yang, H. Xia, B.-R. Gao, J. Feng, Y.-G. Ma and H.-B. Sun, J. Phys. Chem. C, 2010, **114**, 11958-11961.

39 J. Kunzelman, M. Kinami, B. R. Crenshaw, J. D. Protasiewicz and C. Weder, *Adv. Mater.*, 2008, **20**, 119-122.

40 C. Dou, L. Han, S. Zhao, H. Zhang and Y. Wang, *J. Phys. Chem. Lett.*, 2011, **2**, 666-670.

41 Y. Zhang, G. Zhuang, M. Ouyang, B. Hu, Q. Song, J. Sun, C. Zhang, C. Gu, Y. Xu and Y. Ma, *Dyes Pigments*, 2013, **98**, 486-492.

42 R. Davis, N. S. Saleesh Kumar, S. Abraham, C. H. Suresh, N. P. Rath, N. Tamaoki and S. Das, J. Phys. Chem. C, 2008, **112**, 2137-2146.

43 S. J. Yoon, J. H. Kim, K. S. Kim, J. W. Chung, B. Heinrich, F. Mathevet, P. Kim, B. Donnio, A. J. Attias, D. Kim and S. Y. Park, *Adv. Funct. Mater.*, 2012, **22**, 61-69.

44 J. W. Park, S. Nagano, S. J. Yoon, T. Dohi, J. Seo, T. Seki and S. Y. Park, *Adv. Mater.*, 2014**, 26,** 1354-1359.

45 J. Tsibouklis, P. H. Richardson, A. M. Ahmed, R. W. Richards, W. J. Feast, S. J. Martin, D. D. C. Bradley and M. Warner, *Synth. Met.*, 1993, **61**, 159-162.

46 H. Aoki, T. Mihara and N. Koide, *Mol. Cryst. Liq. Cryst.*, 2004, **408**, 53-70.

47 R. Bao, M. Pan, J. J. Qiu and C. M. Liu, *Chin. Chem. Lett.*, 2010, **21**, 682-685.

48 R. Bao, M. Pan, Y. Zhou, J. J. Qiu, H. Q. Tang and C. M. Liu, *Synth. Commun.*, 2012, **42**, 1661-1668.

49 W. Mao, K. Chen, M. Ouyang, J. Sun, Y. Zhou, Q. Song and C. Zhang, *Acta Chim. Sinica*, 2013, **71**, 613-618.

50 S. M. Morris, M. M. Qasim, D. J. Gardiner, P. J. W. Hands, F. Castles, G. Tu, W. T. S. Huck, R. H. Friend and H. J. Coles, *Opt. Mater.*, 2013, **35**, 837-842.

51 R. Wei, Y. He, X. Wang and P. Keller, *Macromol. Rapid Commun.*, 2014, **35**, 1571-1577.

52 V. Percec, A. De Souza Gomes and M. Lee, *J. Polym. Sci., Part A: Polym. Chem.*, 1991, **29**, 1615-1622.

53 H. Lu, S. Zhang, A. Ding, M. Yuan, G. Zhang, W. Xu, G. Zhang, X.-. Wang, L. Qiu and J. Yang, *New J. Chem.*, 2014, **38**, 3429-3433.

54. H. Lu, L. Qiu, G. Zhang, A. Ding, W. Xu, G. Zhang, X. Wang, L. Kong, Y. Tian and J. Yang, *J. Mater. Chem. C*, 2014, 2, 1386-1389.

55 M. Martínez-Abadía, B. Robles-Hernández, B. Villacampa, M. R. de la Fuente, R. Giménez, M. B. Ros, *J. Mater. Chem. C*, 2015, DOI: 10.1039/C5TC00201J.

56 T. Niori, T. Sekine, J. Watanabe, T. Furukawa and H. Takezoe, *J. Mater. Chem.*, 1996, **6,** 1231-1233.

57 G. Pelzl, S. Diele and W. Weissflog, *Adv. Mater.*, 1999, **11,** 707-724.

58 D. M. Walba, in *Materials-Chirality*, eds. M. M. Green, R. J. M. Nolte, E. W. Meijer , S. E. Denmark and J. Siegel, Wiley, New York, 2003, vol. 24 of Top. Stereochem., ch. 8, pp. 457-518.

59 M. Hird, *Liq. Cryst. Today*, 2005, **14**, 9-21.

60 R. A. Reddy and C. Tschierske, *J. Mater. Chem.*, 2006, 16, 907-961.

61 H. Takezoe and Y. Takanishi, *Jpn. J. Appl. Phys., Part 1*, 2006, **45**, 597-625.

62 W. Weissflog, H. N. S. Murthy, S. Diele and G. Pelzl, *Philos. Trans. R. Soc. A*, 2006, **364**, 2657-2679.

63 A. Jákli, C. Bailey and J. Harden, in *Thermotropic Liquid Crystals*, ed. A. Ramamoorthy, Springer Berlin, 2007, ch. 2, pp. 59-83.

64 G. Pelzl and W. Weissflog, in *Thermotropic Liquid Crystals*, ed. A. Ramamoorthy, Springer Berlin, 2007, ch. 1, pp. 1-58.

65 A. Eremin and A. Jákli, *Soft Matter*, 2013, **9**, 615-637.

66 A. Jákli, *Liq. Cryst. Rev.*, 2013, **1**, 65-82.

67 C. Tschierske, *Angew. Chem. Int. Ed.*, 2013, **52**, 8828-8878.

68 *Handbook of Liquid Crystals*, J. W. Goodby, P. J. Collings, T. Kato, C. Tschierske, H. Gleeson and P. Raynes, eds., Wiley-VCH, Weinheim, 2014.

69 M. B. Ros, J. L. Serrano, M. R. de la Fuente and C. L. Folcia, *J. Mater. Chem.*, 2005, **15**, 5093-5098.

70 J. Etxebarria and M. B. Ros, *J. Mater. Chem.*, 2008, **18**, 2919-2926.

71 C. Zang, N. Diorio and A. Jákli, in *Handbook of Liquid Crystals*, eds. J. W. Goodby, P. J. Collings, T. Kato, C. Tschierske, H. Gleeson and P. Raynes, WILEY-VCH, Weinheim, 2014, vol. 4, pp. 715-742.

72 A. Jákli, I. C. Pintre, J. L. Serrano, M. B. Ros and M. R. de la Fuente, *Adv. Mater.*, 2009, **21**, 3784-3788.

73 A. C. Charif, N. Diorio, K. Fodor-Csorba, J. E. Puskas and A. Jakli, *Rsc Advances*, 2013**, 3**, 17446-17452.

74 R. Macdonald, F. Kentischer, P. Warnick and G. Heppke, *Phys. Rev. Lett.*, 1998, **81**, 4408-4411.

75 F. Kentischer, R. Macdonald, P. Warnick and G. Heppke, *Liq. Cryst.*, 1998, **25**, 341-347.

76 C. L. Folcia, I. Alonso, J. Ortega, J. Etxebarria, I. Pintre and M. B. Ros, *Chem. Mater.*, 2006, **18**, 4617-4626.

77 I. C. Pintre, N. Gimeno, J. L. Serrano, M. B. Ros, I. Alonso, C. L. Folcia, J. Ortega and J. Etxebarria, *J. Mater. Chem.*, 2007, **17**, 2219-2227.

78 I. C. Pintre, J. L. Serrano, M. B. Ros, J. Martinez-Perdiguero, I. Alonso, J. Ortega, C. L. Folcia, J. Etxebarria, R. Alicante and B. Villacampa, *J. Mater. Chem.*, 2010, **20**, 2965-2971.

79 B. Champagne, J. Guthmuller, F. Perreault and A. Soldera, *J. Phys. Chem. C*, 2012, **116**, 7552-7560.

80 N. G. Nagaveni, A. Roy and V. Prasad, *J. Mater. Chem.*, 2012, **22**, 8948-8959.

81 H. Ocak, B. Bilgin-Eran, M. Prehm and C. Tschierske, *Soft Matter*, 2012**, 8,** 3773-3783.

82 M. Alaasar, M. Prehm, M. Brautzsch and C. Tschierske, *J. Mater. Chem. C*, 2014, **2**, 5487-5501.

View Article Online
DOI: 10.1039/C5CP00696A

83 N. Gimeno and M. B. Ros, *Handbook of Liquid Crystals*, J. W. Goodby, P. J. Collings, T. Kato, C. Tschierske, H. Gleeson and P. Raynes, eds., Wiley-VCH, Weinheim, 2014. vol. 4, pp. 605-679.
84 J. Gierschner, L. Lüer, B. Milián-Medina, D. Oelkrug and H.-J. Egelhaaf, *J. Phys. Chem. Lett.*, 2013, **4**, 2686-2697.
85 J. Shi, S.-J. Yoon, S. Varghese, B. Milián-Medina, S. Y. Park, J. Gierschner, *In preparation*.
86 J. Gierschner, H.-G. Mack, L. Lüer and D. Oelkrug, *J. Chem. Phys.*, 2002, **116**, 8596-8609.
87 M. Kasha, H. R. Rawls, M. A. El-Bayoumi, *Pure Appl. Chem.*, 1965, **11**, 371-392.
88 J. Cornil, D. Beljonne, J. P. Calbert and J. L. Brédas, *Adv. Mater.*, 2001, **13**, 1053-1067.
89 F. C. Spano, *J. Chem. Phys.*, 2001, **114**, 5376-5390.
90 H. J. Egelhaaf, J. Gierschner and D. Oelkrug, *Synth. Met.*, 2002, **127,** 221-227.
91 S. Strickler and R. A. Berg, J. Chem. Phys., 1962, **37**, 814-822.
92 J. P. Vikesland and S. J. Strickler, *J. Chem. Phys.*, 1974, **60**, 660-663.
93 Gaussian 09, M. J. Frisch, G. W. Trucks, H. B. Schlegel, G. E. Scuseria, M. A. Robb, J. R. Cheeseman, G. Scalmani, V. Barone, B. Mennucci, G. A. Petersson, H. Nakatsuji, M. Caricato, X. Li, H. P. Hratchian, A. F. Izmaylov, J. Bloino, G. Zheng, J. L. Sonnenberg, M. Hada, M. Ehara, K. Toyota, R. Fukuda, J. Hasegawa, M. Ishida, T. Nakajima, Y. Honda, O.Kitao, H. Nakai, T. Vreven, J. A. Jr. Montgomery, J. E. Peralta, F. Ogliaro, M. Bearpark, J. J. Heyd, E. Brothers, K. N. Kudin, V. N. Staroverov, R. Kobayashi, J.Normand, K. Raghavachari, A. Rendell, J. C. Burant, S. S. Iyengar, J. Tomasi, M. Cossi, N. Rega, J. M. Millam, M. Klene, J. E. Knox, J. B. Cross, V. Bakken, C. Adamo, J. Jaramillo, R. Gomperts, R. E. Stratmann, O. Yazyev, A. J. Austin, R. Cammi, C. Pomelli, J. W. Ochterski, R. L. Martin, K. Morokuma, V. G. Zakrzewski, G. A. Voth, P.Salvador, J. J. Dannenberg, S. Dapprich, A. D. Daniels, Ö. Farkas, J. B. Foresman, J. V. Ortiz, J. Cioslowski, D. J. Fox, Gaussian, Inc., Wallingford CT, 2009.